

***REVISED** Technical Briefs Manuscript submitted to ASME J. Heat Transfer*

# **A New Finite-Conductivity Droplet Evaporation Model Including Liquid Turbulence Effect**

**M. S. Balasubramanyam, C. P. Chen\***

cchen@che.uah.edu

Department of Chemical and Materials Engineering  
University of Alabama in Huntsville, Huntsville  
Huntsville, Alabama 35899

**H. P. Trinh**

Engineering Directorate  
NASA-Marshall Space Flight Centre  
Huntsville, Alabama 35812

\*Corresponding Author

Keywords: Evaporation, Spray, Numerical Modeling

A new approach to account for finite thermal conductivity and turbulence effects within atomizing droplets of an evaporating spray is presented in this paper. The model is an extension of the T-blob and T-TAB atomization/spray model of Trinh and Chen [9]. This finite conductivity model is based on the two-temperature film theory in which the turbulence characteristics of the droplet are used to estimate the effective thermal diffusivity for the liquid-side film thickness. Both one-way and two-way coupled calculations were performed to investigate the performance of this model against the published experimental data.

## Introduction

Spray vaporization and combustion studies are of primary importance in the prediction and improvement of systems utilizing spray injection. In liquid fuelled combustion systems such as industrial boilers, gas turbines, direct ignition diesel engines, rocket and air-breathing engine applications, the combustion performance is highly dependent on effective liquid fuel atomization and its subsequent evaporation processes. The recent review by Sazhin [1] had summarized the development of various droplet heat-up and evaporation models with different levels of complexity. As also pointed out in [1], to numerically simulate evaporating spray using CFD (computational fluid dynamics) methodologies, detailed droplet heating and evaporation models based on single-droplet analysis have to be simplified to be CPU efficient. Although the film-theory based evaporation models had been extensively used, most of the developments were done on the gas-side heat and mass transfer [2, 3]. Within the liquid droplet, the two-temperature formulations, in which the finite-conductivity (F-C) effect was modelled by the temperature difference between the droplet surface temperature and a droplet “core” temperature have been proposed recently. In the model of Renksizbulut et al. [4], the difference between the surface and core temperature was related to the heat flux at the droplet surface by a constant Nusselt number. Zeng and Lee [5] developed a zero-dimensional model, in which the difference between surface and core temperature was traced by an ordinary differential equation (ODE) to account for the non-uniform distribution of temperature inside the droplet. The ODE two-temperature model was also used by Miller et al. [6] to account for

non-equilibrium Langmuir-Knudsen mass transfer effect. Ra and Reitz [7] used a thermal boundary layer within the droplet to account for the finite-conductivity effect. The thermal boundary layer thickness was calculated using the thermal diffusivity model of Abramzon and Sirignano [8] to account for the droplet internal circulation.

In this paper, a new finite-conductivity model is developed upon the two-temperature formulation. The finite-conductivity effect is phenomenologically modelled through a thermal boundary layer within the droplet. The thermal diffusivity is calculated based on the turbulent characteristics within the droplet. The current study is an extension of a recently developed atomization/spray model [9, 10], the T-blob/T-TAB model, to include spray evaporation effects. Due to the unique feature of T-blob/T-TAB, in which the turbulence characteristics is accounted for within the droplet phase, extension of this model to include finite conductivity effect in the evaporating droplet can be made naturally. The model development will be described in this paper. Validations for one-way one-dimensional and two-way coupled multi-dimensional evaporating sprays will be presented.

## **Model Development**

The current vaporization model is developed for computational analysis based on the Eulerian-Lagrangian numerical approach. In this formulation, the spray/droplets dynamics is described in a Lagrangian coordinate such that numerical droplets are tracked within the Eulerian gas dynamics. Liquid phase is tracked from the injector plane, and the primary atomization as well as the subsequent secondary break-up is modelled using the T-blob/T-TAB hybrid model of Trinh and Chen [9]. Both primary and secondary droplet break-up processes are modelled and the transition from primary to secondary break-up is modelled based on an energy balance. In addition to the droplets position and velocity, liquid turbulence is accounted for through the injector characteristics by the two-equation  $k$ - $\epsilon$  turbulence model formulation using the T-blob/T-TAB model. The inherent turbulence in the injected fuel spray affects the heat and mass transfer rates of the vaporization process. The effects of these changes in the rates have to be accounted for in the

numerical models for spray evaporation. Detailed model description and validations can be found in [9, 10], and it is sufficient to say that within each numerical droplet, turbulence characteristics such as fluctuating velocity level, length and time scales are supplied by the model.

To utilize the T-blob/T-TAB model liquid jet atomization, turbulence characteristics need to be specified as the inlet boundary conditions. Based on integral analysis of straight injector [9], liquid turbulent kinetic energy and its dissipation rate at the injector nozzle exit are estimated from:

$$k_l^o = \frac{U^2}{8L/D_{nozzle}} \left[ \frac{1}{C_d^2} - K_c - (1 - s^2) \right] \quad (1)$$

$$\varepsilon_l^o = K_\varepsilon \frac{U^3}{2L} \left[ \frac{1}{C_d^2} - K_c - (1 - s^2) \right], \quad (2)$$

where  $L$  is the length of the injector nozzle,  $D_{nozzle}$  is the nozzle diameter, and the jet injection velocity  $U$ . A set of ODE's were derived to track the evolution of  $k_l$  and  $\varepsilon_l$  within the droplet according to the T-blob/T-TAB model. The values obtained from the evolution of  $k_l$  and  $\varepsilon_l$  are used in the heat transfer calculations of the evaporation droplet.

To relax the infinite-conductivity assumption, and thus perfect mixing within the liquid droplet, a “two-temperature” model is formulated. In the two-temperature model, the core (or bulk) temperature ( $T_d$ ), is assumed to be well-mixed by convection/turbulence transport. Consistent with the “film theory”, heat resistance exists at the near surface region, and the droplet surface temperature ( $T_s$ ) differs from the droplet core temperature. The heat transfer coefficient across this thin film (or boundary layer) is then formulated through the turbulence characteristics supplied from the T-blob/T-TAB model, to account for the finite conductivity effect. In the Lagrangian coordinate, the heat-up of the droplet core is formulated as:

$$m_d C_p \frac{dT_d}{dt} = h_l (T_s - T_d) A_d \quad (3)$$

where,  $h_l$  is the liquid-side heat transfer coefficient and  $A_d$  is the droplet surface area. The heat transfer coefficient is determined from the thermal conductivity and a thermal boundary layer formulation [11] as:

$$h_l = \frac{\lambda_l}{\delta_e}, \quad (4)$$

where  $\lambda_l$  is the liquid thermal conductivity. Using an unsteady equivalent boundary layer thickness, the film thickness,  $\delta_e$ , is given by  $\sqrt{\pi \alpha_{eff} t}$ . The time scale  $t$  is estimated based on the heat transfer-limited integration time step, and should be independent of the global time step used in numerical calculations (see the results in figure 1). In this study, we adopted the evaporation sub-cycle time step based on the formulation described in Amsden et al. [12]. This time step is computed by the relation given by:

$$t = \frac{\rho_g dV}{\mu_g Sh_g (4\pi r_d) N_p}, \quad (5)$$

where  $dV$  is the volume of the computational cell,  $\rho_g$  is density,  $\mu_g$  is the viscosity of gas mixture within the cell, and  $N_p$  is the number of droplets for each computational particle  $p$ . The effective thermal diffusivity ( $\alpha_{eff}$ ), based on the turbulence characteristics within the droplet, is estimated from:  $\alpha_{eff} = \alpha_{lam} + \alpha_{urb}$ , in which the turbulent thermal diffusivity is calculated from the two-equation turbulence model diffusivity formulation:

$$\alpha_{urb} = \frac{C_\mu k_l^2}{Pr_t \varepsilon_l}, \quad (6)$$

here,  $Pr_t$  is the turbulent Prandtl number and is set to be 0.9. The liquid droplet turbulence quantities  $k_l$  and  $\varepsilon_l$  are obtained from the T-blob/T-TAB atomization/spray model. In cases where gas phase diffusivities are much larger than liquid diffusivities, the droplet core heating will be rate controlling and the gas-side heat/mass transfer will respond in a quasi-steady manner. The surface temperature of the droplet is determined from a heat and mass transfer balance at the interface between the droplet and the surrounding gas assuming no heat accumulation at the droplet surface such that:

$$L_v \dot{m}_d = q_g - q_l \quad (7)$$

where  $L_v$  is the latent heat of the fuel at the surface temperature, and  $q_g$  is the heat transfer rate from the environmental gas to the surface. In this paper, the classical Spalding evaporation model is used to model the gas-phase transport, thus the gas heat transfer rate was calculated as:

$$q_g = 2\pi r_d \lambda_g Nu_g (T_g - T_s) \frac{\ln(1 + B_T)}{B_T} \quad (8)$$

$q_l$  in Eq. (7) is the heat transfer rate from the droplet interior to droplet surface, and is calculated from:

$$q_l = \frac{\lambda_l (T_s - T_d)}{\delta_e} A_d \quad (9)$$

The evaporation rate at the droplet surface is given as:

$$\dot{m}_d = \frac{dm_d}{dt} = 2\pi r_d (\rho_g \bar{D}) Sh_g \ln(1 + B_m) \quad (10)$$

In the above equation,  $B_m$  is the Spalding mass transfer number,  $Sh_g$  is the Sherwood number, and  $\bar{D}$  is the binary diffusivity. The Sherwood and the Nusselt numbers were calculated using the classical correlations give by:

$$Nu_g = 2 + 0.6 Re_p^{0.5} Pr^{0.333} \quad (11)$$

$$Sh_g = 2 + 0.6 Re_p^{0.5} Sc^{0.333} \quad (12)$$

The solution algorithm used in this study starts with an estimated surface temperature ( $T_s$ ) at a new time step. The Clausius-Clayperon equation and the Raoult's law are then used to calculate the fuel vapour molar fraction followed by the calculation of the evaporation rate. An estimation of  $T_d$  is also required to simultaneously satisfy Eqs. (3) and (7). A more detailed iterative procedure can be found in Balasubramanyam [13].

## Results and Discussion

### One-Way Evaporating Atomizing Spray

In one-way simulation, the gas flow field was prescribed and the droplets were tracked in time domain. This case is an extension of the one-way T-blob/T-TAB testing case described in Trinh and

Chen [9]. Iso-octane fuel similar to the fuel used in reference [7] was issued through a long injector tube at 300°K. The length of the injector nozzle ( $L$ ) is 0.8 mm and the nozzle diameter ( $D_{\text{nozzle}}$ ) is 0.3 mm. A jet injection velocity ( $U$ ) of 102 m/s was used for the test case. The environment is quiescent nitrogen at a temperature of 600°K. The gas properties were calculated based on the reference state determined from the '1/3<sup>rd</sup>' rule [11]. In this calculation, a 'blob' of numerical droplet was injected at the orifice plane with orifice diameter. The droplet then went through the primary and secondary break-up processes, thus its diameter decreased with time. The variation of the thermal boundary layer within the droplet also changed with time. The purpose here is to investigate the concept of boundary layer film thickness within liquid droplets involving two temperatures. In the course of study, it was found that in the secondary break-up regime (i.e. the T-TAB regime) the droplets were so small they were heated up rapidly. Thus the current model was only implemented within the T-blob (i.e., the primary break-up) model. Figure 1 shows the history of the normalized effective film thickness within the liquid droplets. The results indicate that the normalized thermal boundary layer thickness is rather thick in the initial stage, and then decreases quickly to a small value exhibiting a reasonable physical trend. It should be noticed that the current model gives thinner thermal boundary layer thickness when compared with the limiting thermal layer thickness based on internal vortex convection model. Utilizing the model of Abramzon and Sirignano [8], Ra and Reitz [7] suggested that the value of thermal layer thickness be limited to 1/2.257 of the droplet radius. It was also observed that, based on the current model, the turbulent diffusivity within the droplet was at least one order of magnitude greater than the laminar thermal diffusivity. The turbulent thermal diffusivity decreased in tandem with the decrease in the kinetic energy experienced by the drop. The variation of the drop surface temperature ( $T_s$ ) and the bulk temperature of the drop ( $T_d$ ) for the finite conductivity (F-C) model in comparison with the bulk temperature calculated using the infinite conductivity (I-C) model is shown in Fig. 2. The temperature profiles for  $T_d$  and  $T_s$  were in close comparison to the results obtained by reference [7] for iso-octane evaporation. The variation of the normalized parent drop radius with time for a one-

way coupled test case, with iso-octane fuel evaporating in a quiescent environment is shown in figure 3. The present F-C model predicted a higher rate of change in the droplet radius (i.e. shorter droplet life time) than the I-C model due to the higher droplet surface temperature (see Fig. 2), which gave a higher evaporation rate. The results of this comparison indicated that the droplet lifetimes predicted by the finite conductivity model are shorter than the prediction by the infinite conductivity model. The reason for this is due to droplet radius being evaluated based on the droplet surface temperature, which is higher than the interior temperature in the case of the evaporating droplet. The difference in rates increases with an increase in ambient temperature. The current model compares favourably with the models of Refs. [5] and [7]. The next step in the numerical development of the model was to validate its efficiency for applications in practical situations. To this effect, the model was then incorporated into the finite volume CFD code ACE+ [14] for two-way coupled validation study using the Eulerian-Lagrangian methodology [15]. In the two-way simulation, mutual interaction between the gas phase and the evaporating spray were accounted for by extra source terms in the equations of change for mass and momentum. The detailed numerical implementation, as well as grid size and time steps issues, can be found in Balasubramanyam [13].

### **Two-Way Coupled Evaporating Spray Validation**

To evaluate the current evaporation model, the 2-D axis-symmetric subsonic low-evaporating spray of Yakota et al. [16] was tested for a two-way coupling CFD calculation since a similar non-evaporating test case was used for the T-blob/T-TAB validation study [10]. Liquid fuel (Tridecane,  $C_{13}H_{28}$ ) is injected through a single-hole nozzle into a pressurized, high temperature ambient  $N_2$  environment. The test conditions for the evaporating spray are summarized in Table 1. The nozzle diameter was 0.16 mm. Eqs. (1) and (2), with the same values for nozzle parameters except for nozzle diameter and jet velocity, were used to estimate the initial liquid turbulence quantities. A computational domain of 20 mm in radius and 100 mm in length discretized by a 50 radial x 75 axial grid was used. The mesh spacing was non-uniform with refinement on the centreline and close to the injector. A constant time step of 2.5E-6 sec. was used with an injection



period of 4  $\mu$ sec. The properties of liquid fuel Tridecane were taken from the NIST/JANAF database. Estimating the penetration of a fuel jet into an air stream is an important global property for model validation and is presented first. In Fig. 4, the predicted tip penetration results using the current finite-conductivity (F-C) evaporation model coupled with the T-blob/T-TAB atomization model are compared with the measured data. For reference, predictions using classical Blob/TAB/infinite-conductivity (I-C) model, as well as using T-blob/T-TAB/infinite-conductivity model are also shown in the same figure. As indicated in [16], the infinite-conductivity evaporation models tend to over-predict the evaporation rate for multi-dimensional two-way coupled calculations, thus gave shorter tip penetration. On the other hand, the finite-conductivity model slows down the evaporation process, and produces larger droplets and longer penetration. It should be noted that the coalescence model [10] was used for all two-way coupling calculation cases. The coalescence model is responsible for the calculated overshoot phenomena observed in the initial period of injection for all simulated cases. In the downstream region, the current model gives much better comparison with the experimental data. The heat transfer aspects of the evaporating jet are shown in Fig. 5 at time of 4  $\mu$ sec after injection. As can be observed, the models incorporating the turbulence effects in the primary and secondary atomization processes give more reasonable qualitative pictures when compared with the classical atomization model without liquid turbulence effect. Comparing Figs. 5.(b) and 5.(c), the surface temperature contours predicted by the current finite-conductivity model show the effect of slowing down the rate of evaporation, and qualitatively compared well with the more sophisticated droplet heat-up model of Bertoli and Migliaccio [17].

## Concluding Remarks

Based on the two-temperature film theory, a new finite-conductivity model accounting for droplet internal turbulence effect is developed for evaporating spray numerical calculations. The model is an extension of the existing T-blob/T-TAB atomization/spray model which provides the turbulence characteristics for estimating an effective thermal diffusivity within the droplet. Based on the one-way simple spray results, the model exhibits reasonable physical trends in terms of

droplets evaporation features. The current model can be efficiently incorporated into practical spray combustion CFD codes. In two-way Eulerian-Lagrangian multi-dimensional full CFD simulations utilizing CFD-ACE+ code, the current finite-conductivity model coupled with the T-blob/T-TAB model shows superior performance to the conventional infinite-conductivity evaporation model, by comparison to evaporating spray experimental data.

## Acknowledgements

This study was partially supported by NASA Grant NCC8-200 through the UAH Propulsion Research Centre. The authors would also like to acknowledge the use of the CFD-ACE+ code under an educational agreement with CFD Research Corporation.

## Nomenclature

$A_d$	Droplet surface area ( $m^2$ )
$B_m$	Gas phase mass transfer number
$C_d$	Discharge coefficient of injector nozzle (0.07 in this study)
$C_p$	Specific heat capacity of mixture(KJ/kg K)
$C_\mu$	Turbulence constant
$\bar{D}$	Binary Diffusivity ( $m^2/s$ )
$K_c$	Loss coefficient due to nozzle inlet geometry (0.45)
$K_\epsilon$	Proportionality constant (0.23)
$k_l$	Turbulent kinetic energy of the liquid ( $m^2/s^2$ )
$L_v$	Latent heat of the fuel at surface temperature (KJ/kg)
$m_d$	Droplet mass (kg)
$Nu_g$	Gas phase Nusselt number
$Pr_t$	Turbulent Prandtl number (0.9)
$P_{atm}$	Atmospheric pressure (Pa)
$P_{gas}$	Gas phase pressure (Pa)
$q_l$	Heat transfer rate from droplet surface to droplet core
$q_g$	Heat transfer rate from gas phase to droplet surface
$r_d$	Droplet radius (m), $D_p$ is diameter
$Sh_g$	Gas phase Sherwood number
$T_b$	Fuel boiling temperature (K)
$T_d$	Bulk temperature of droplet (K)
$T_g$	Ambient gas temperature (K)
$T_s$	Droplet surface temperature (K)
$s$	Area ratio at nozzle contraction, (0.0 in this study)

$U$	Droplet injection velocity (m/s)
$\alpha_{\text{eff}}$	Effective thermal diffusivity ( $\text{m}^2/\text{s}$ )
$\alpha_{\text{lam}}$	Laminar thermal diffusivity ( $\text{m}^2/\text{s}$ )
$\alpha_{\text{urb}}$	Turbulent thermal diffusivity ( $\text{m}^2/\text{s}$ )
$\lambda_l$	Liquid thermal conductivity
$\lambda_g$	Gas thermal conductivity (KW/m K)
$\epsilon_1$	Turbulent dissipation rate ( $\text{m}^2/\text{s}^3$ )
$\delta_e$	Equivalent thickness of thermal boundary layer

## References

1. Sazhin, S. S., 2006, "Advanced Models of Fuel Droplet Heating and Evaporation," *Prog. Energy and Combustion*, 32, pp. 162-214.
2. Yao, G. F., "A Film-Theory-Based Model for a Multicomponent Droplet Evaporation at both Low and High-Pressure Environments," 2006, *ASME J. Heat Transfer*, 128, pp. 290-294.
3. Wu, J. S., Hsu, K.-H., Kuo, P.-M., and Sheen, H. J., "Evaporation Model of a Single Hydrocarbon Fuel Droplet due to Ambient Turbulence at Intermediate Reynolds Numbers," 2003, *Int. J. Heat Mass Transfer*, 46, pp. 4741-4745.
4. Renksizbulut, M., Bussmann, M., and Xianguo, L., 1992, A Droplet Vaporization Model for Spray Calculations, *Particle and Particulate System Characterization*, 9, 59-65.
5. Zeng, Y. and C. F. Lee, 2002, A Model for Multicomponent Spray Vaporization in a High-Pressure and High-Temperature Environment, *J. of Eng. for Gas Turbines and Power*, 124, pp. 717-724.
6. Miller, R. S., Harstad, K., and Bellan, J., 1998, Evaluation of Equilibrium and Non-Equilibrium Evaporation Models for Many-Droplet Gas-Liquid Flow Simulations, *Int. Journal of Multiphase Flow*, 24, pp. 1025-1055.
7. Ra, Y. and Reitz, R. D., 2003, The Application of a Multicomponent Droplet Vaporization Model to Gasoline Direct Injection Engines, *Int. J. Engine Research*, 4, pp. 193-218.
8. Abramzon, B. and Sirignano, W. A., 1989, "Droplet Vaporization Model for Spray Combustion Calculations," *Int. J. Heat and Mass Transfer*, 32, 1605-1618.
9. Trinh, H. P. and Chen, C. P., 2006, Modeling of Turbulence Effects on Liquid Jet Atomization and Breakup, accepted to appear in *Atomization and Spray*, also AIAA-2005-0154.
10. Trinh, H. P., Chen, C. P., and Balasubramanyam, M. S., 2005, Numerical Simulation of Liquid Jet Atomization Including Turbulence Effects, accepted, *ASME J. Eng. Gas Turbine*.
11. Sirignano, W. A., 1999, *Fluid Dynamics and Transport of Droplets and Sprays*, Cambridge University Press.
12. Amsden, A. A., O'Rourke, P. J., and Butler, T. D., 1989, "KIVA-II: A Computer Program for Chemically Reactive Flows with Sprays", KIVA LA-11560-MS.
13. Balasubramanyam, M. S., 2006, Modeling Turbulence Effects on the Heat and Mass Transfer of Evaporating Sprays, Ph.D. Dissertation, Department of Mechanical and Aerospace Engineering, University of Alabama in Huntsville.
14. CFD-ACE+, CFD Research Corporation, 2004, ACE+ Theory Manual.
15. Chen, C. P., Shang, H. M. and Jiang, Yu, 1992, "An Efficient Pressure-Velocity Coupling Method for Two-Phase Gas-Droplet Flows," *Int. J. Numerical Method Fluids*, 15, pp. 233-245.
16. Yokota, H., Kamimoto, T., and Kobayashi, H., 1988, A Study of Diesel Spray and Flame by an Image Processing Technique, *Bulletin of JSME*, 54.
17. Bertoli, C. and Migliaccio, M. na., 1999, A Finite Conductivity Model for Diesel Spray Evaporation Computations, *Int. Journal of Heat & Fluid Flow*, 20, 552-561.

Table 1. Test Conditions for the Measurement of Yokota et al. [16]

Case	$P_{inj}$	$P_{gas}$	$T_{amb}$	$M_{inj}$	Gas Environment
Evap. spray	30 Mpa	3 Mpa	900 K	0.00326 kg/s	N <sub>2</sub>

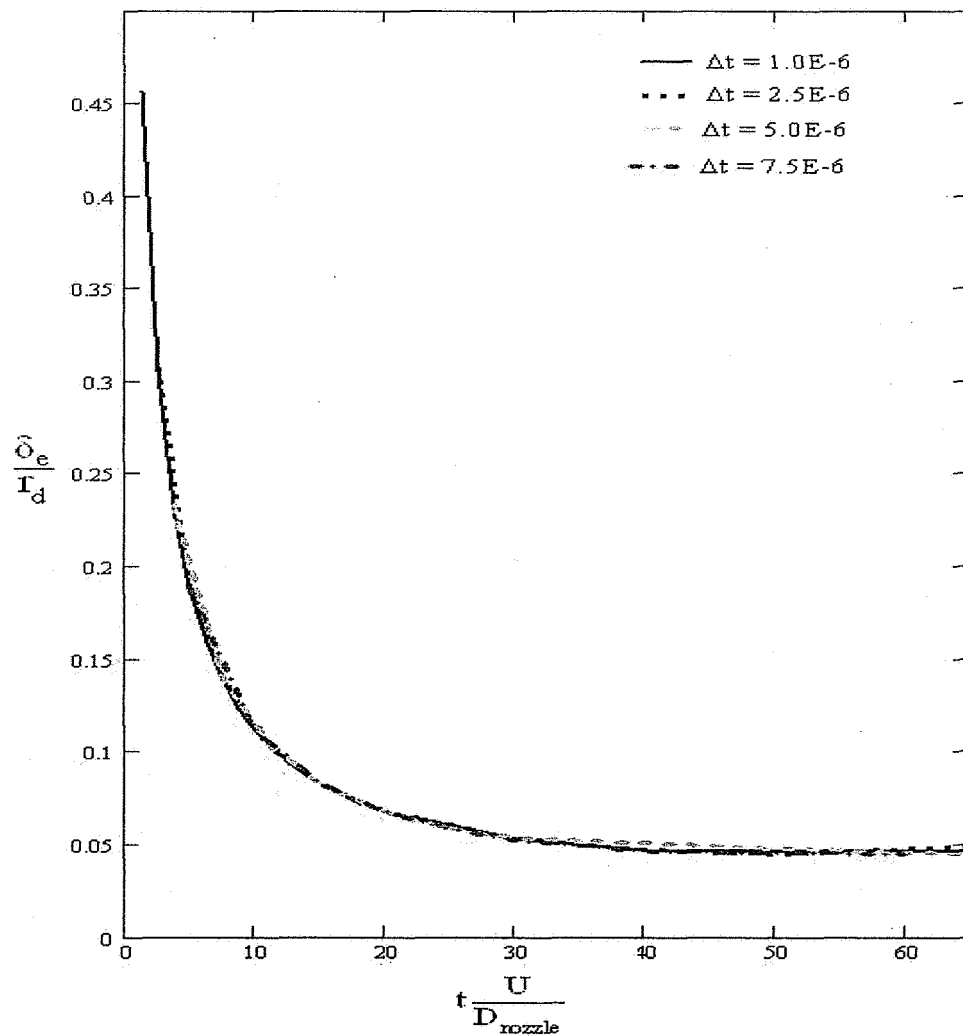


Figure 1. History of effective film thickness within the evaporating droplet using various integration time steps.

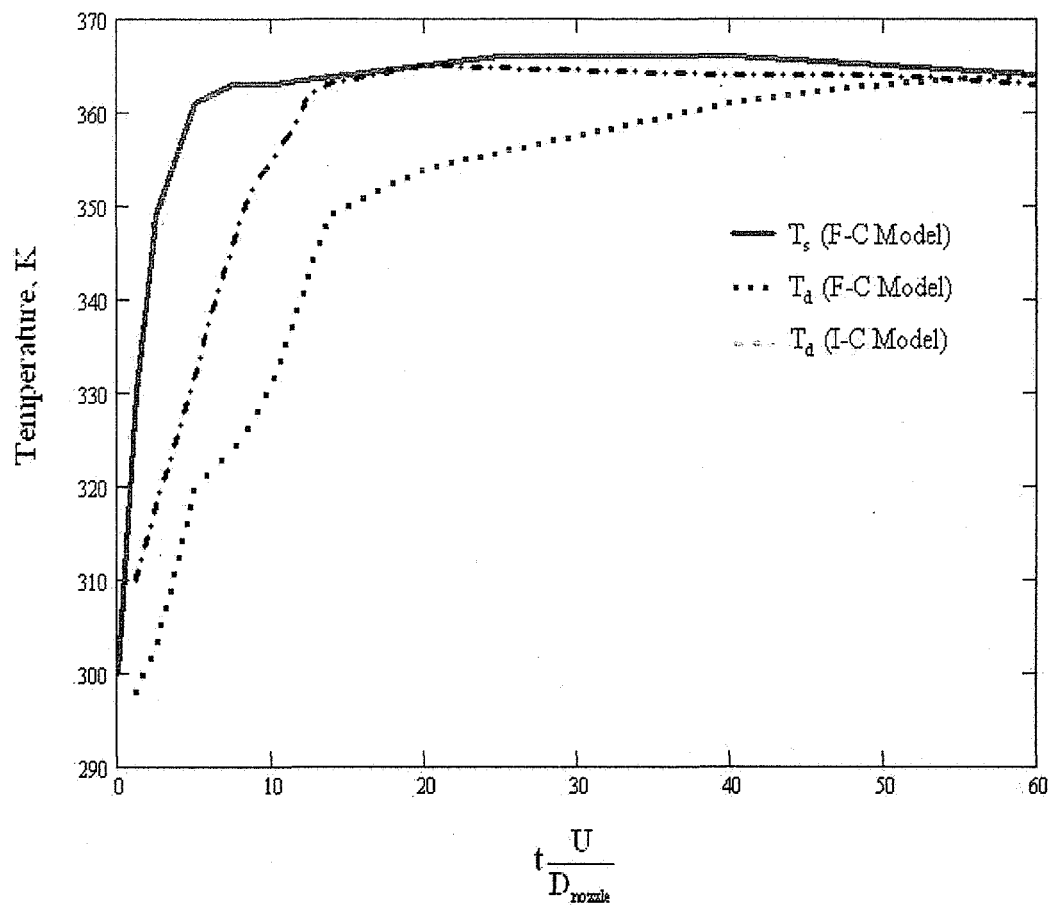


Figure 2. Droplet temperature history comparisons using the current finite-conductivity (F-C) and the infinite-conductivity (I-C) models

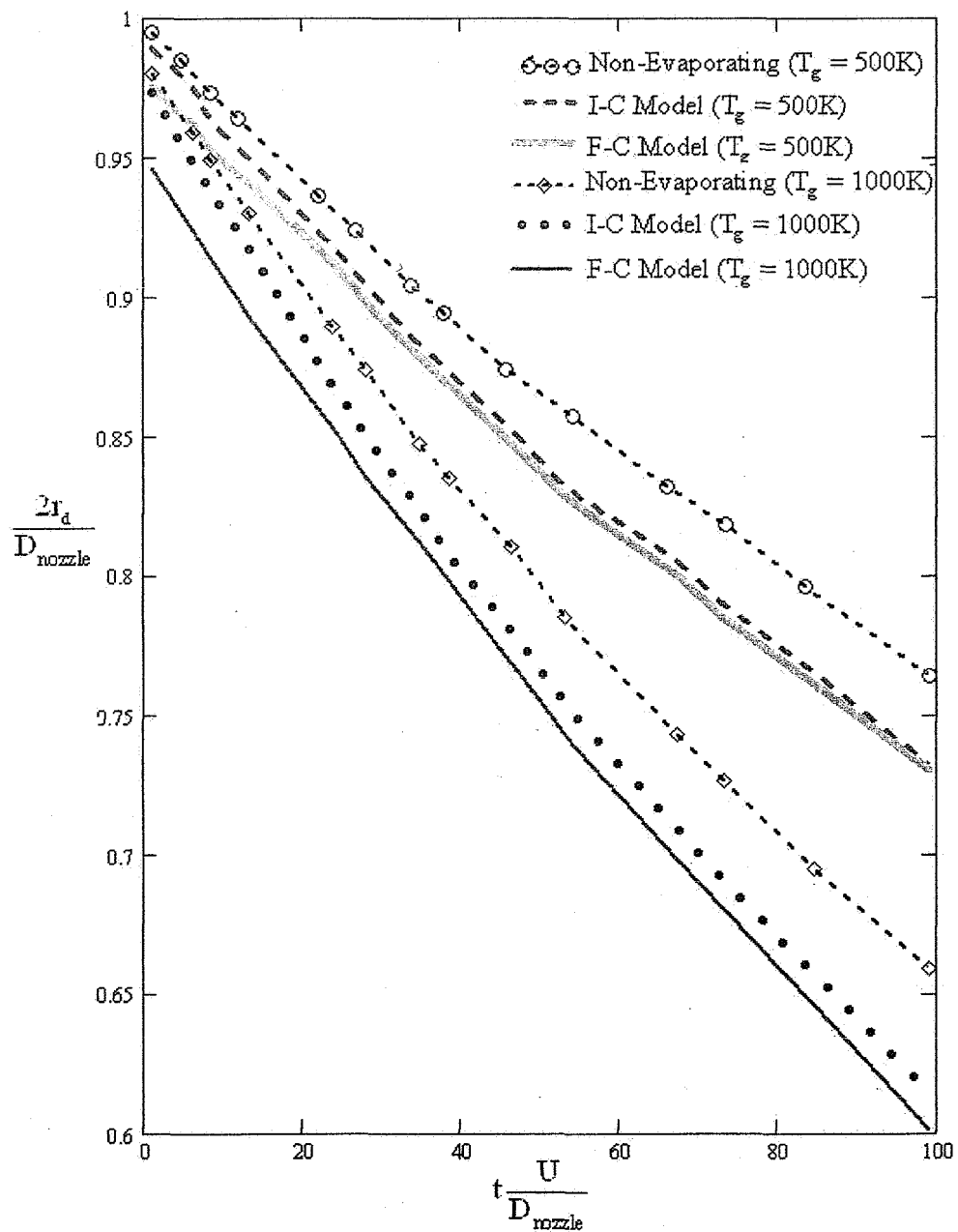


Figure 3. Comparative change in drop size for the F-C and I-C models  
(Non-Evaporating – Atomization without vaporization model)

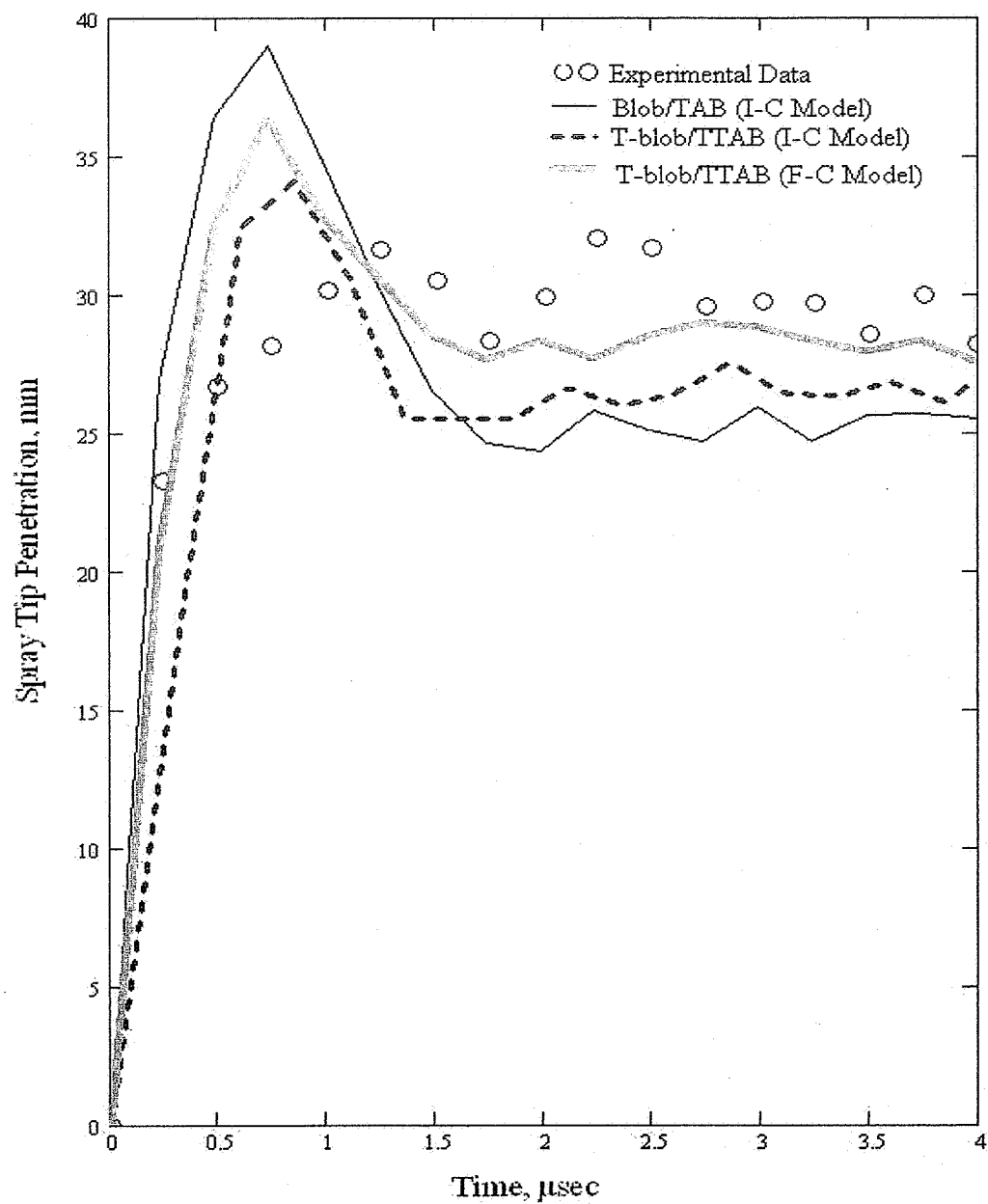


Figure 4. Spray tip penetration with time comparisons using the current F-C model and the infinite-conductivity (I-C) model.

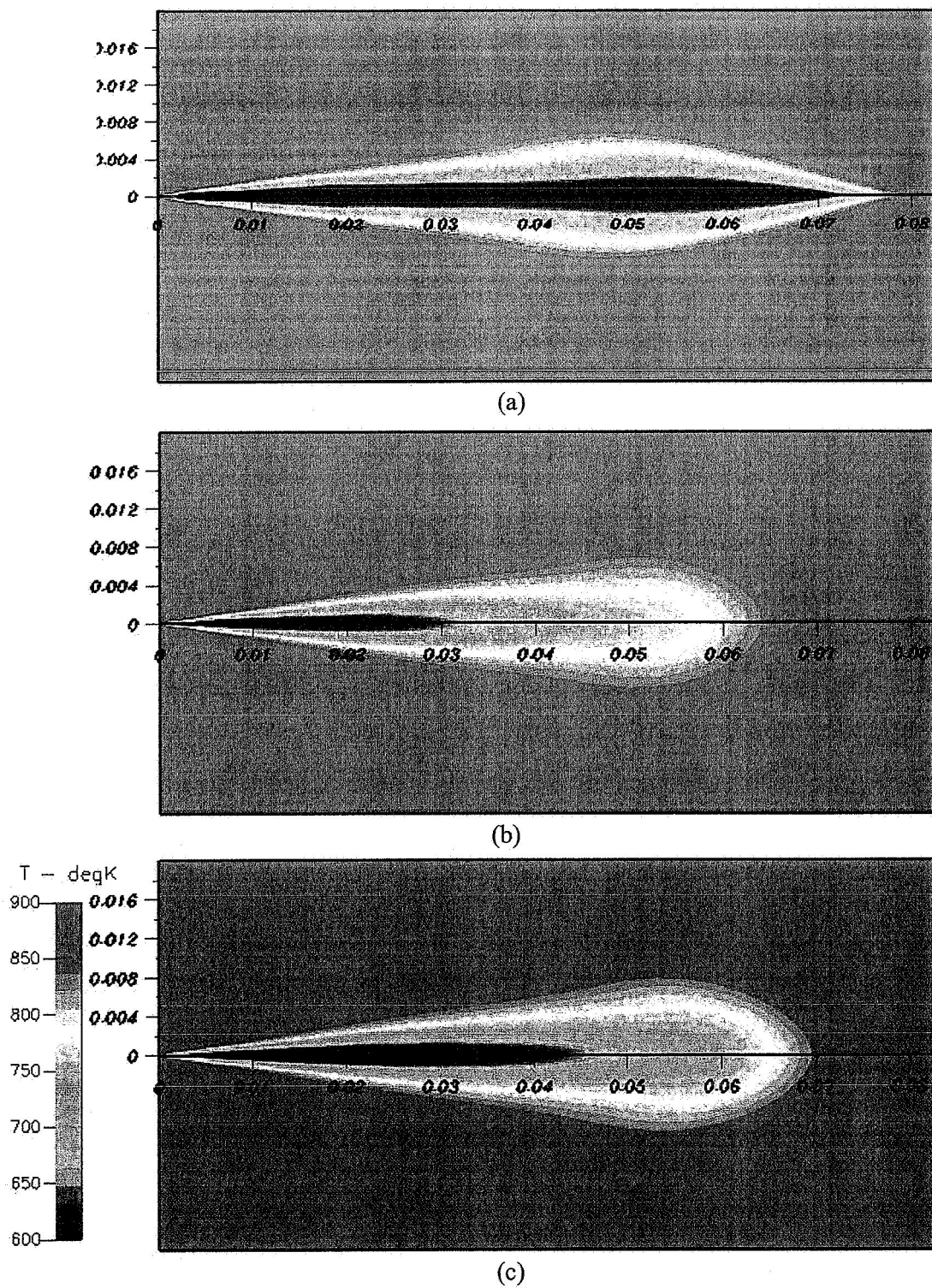


Figure 5. Temperature Contours (X, Y direction in m) at 4  $\mu$ sec; (a) I-C with Blob/TAB, (b) I-C with T-blob/T-TAB, (c) F-C with T-blob/T-TAB